PHYSICAL REVIEW A VOLUME 43, NUMBER 6 15 MARCH 1991

Density-functional theory of surface melting

R. Ohnesorge, H. Löwen, and H. Wagner
Sektion Physik der Universität München, Theresienstrasse 37, D-8000 München 2, Federal Republic of Germany
(Received 22 March 1990; revised manuscript received 8 October 1990)

A microscopic theory of planar crystal surface melting is described and applied to rare gases with Lennard-Jones potential. Explicit results for the solid-vapor density profiles are presented that exhibit surface melting in the vicinity of the triple point. Our approach is based on density-functional techniques combined with a van der Waals approximation and a hard-sphere fluid as a reference system.

I. INTRODUCTION

It is a common experience that liquids may easily be undercooled but crystals can hardly be overheated. This disparity between freezing and melting gives a clue that melting initiates at the crystal surface, which is a natural and omnipresent defect in the crystalline order, whereas freezing has to overcome kinetic obstacles of nucleation.

Over the years empirical evidence has accumulated to demonstrate that the melting action is indeed on the surface.[1] In particular, the experiments confirm older ideas[2] that melting of a solid in coexistence with its vapor starts in a continuous fashion well below the triple point and evolves via the growth of a quasiliquid surface layer as the triple point is approached. Accordingly, surface melting is an example of interfacial wetting.

The phenomenon occurs in rare-gas crystals[3] as well as in metals[4–10] and appears to be universal with the qualification that on metals the equilibrium thickness of the molten layer depends sensitively on the lattice orientation of the interface.[4,7] The decisive role of the solid-vapor interface to initiate melting is further underlined by the observation that Ag crystals (melting temperature 1234 K) covered by a thin film of Au (1337 K) can be substantially overheated.[11]

These findings have attracted much attention since they may provide a key for a deeper understanding of the molecular melting mechanism, which is still unsatisfactory. Quantitative aspects of surface melting have been studied by classical phonon theory,[12] lattice models,[13,14] phenomenological Landau theories,[15–18], a Kosterlitz-Thouless approach,[19] and by computer simulations.[20–25]

A first-principles description of interfacial features requires a realistic theory of coexisting bulk phases. Fortunately, this prerequisite is supplied by the density-functional method,[26] which has been developed into a fairly accurate scheme, allowing one to compute equilibrium properties of bulk crystals from those of the fluid.[27–29] In particular, the short-distance structure of the liquid is carried over to the solid phase and the crystalline order is viewed as a condensation of density waves. Recently, we extended this approach[30] to cope with interfaces involving a spatially varying multiple order parameter, such as in quasiliquid wetting layers. In this paper we apply this theory to examine surface melting in Lennard-Jones-type crystals.

In Sec. II we briefly recall the steps leading to a van-der-Waals-type variational expression for the interfacial free energy with the hard-sphere fluid as a reference system. Section III outlines the computation of the coefficient functions in the free-energy functional. We employ the modified weighted-density approximation (MWDA) recently introduced by Denton and Ashcroft.[31] The MWDA is simple to implement and yields satisfactory results for the freezing of hard spheres. However, in the present case the MWDA must be adapted to allow for an unbiased variational calculation of the local order parameters in the interface. The problem is that a weighted-density approximation does not automatically rule out unphysical configurations with overlapping hard spheres.[32].

The treatment of the attractive part in the atomic interaction is described in Sec. IV which also contains the resulting bulk phase diagram. In Sec. V we present our main results for the interfacial profiles displaying surface melting near the triple point. Section VI is a brief summary with some concluding remarks.

II. INTERFACIAL FREE ENERGY

In order to treat the thermostatistics of a strongly inhomogeneous system like a solid-vapor interface, we use the density-functional formalism,[26] which rests upon a variational principle. For a one-component many-body system with volume V, temperature T, and chemical potential μ there exists a unique Gibbs functional, $\Omega(V,T,\mu;[\rho])$ of the single-particle density $\rho(\mathbf{r})$ such that

$$\Omega(V,T,\mu)=\min_{\rho(\mathbf{r})}\Omega(V,T,\mu;[\rho]) \quad (1)$$

equals the grand canonical potential. The minimizing density distribution is the equilibrium distribution within the given boundary conditions supplementing (1).

This variational principle only ensures the existence of $\Omega[\rho]$. As a first step to construct a concrete approximate

expression for $\Omega[\rho]$, we assume a pairwise interatomic potential $\phi(\mathbf{r})=\phi_s(\mathbf{r})+\phi_l(\mathbf{r})$, which we split[30] into a short-range part ϕ_s and a long-range tail ϕ_l. We treat the latter in mean-field approximation, so that

$$\Omega[\rho]=\Omega_s[\rho]+\tfrac{1}{2}\int d^3r\int d^3r'\rho(\mathbf{r})\rho(\mathbf{r}')\phi_l(|\mathbf{r}-\mathbf{r}'|)\ , \tag{2}$$

where Ω_s arises solely from ϕ_s. It is convenient to separate the ideal gas contribution from $\Omega_s[\rho]$ and to define an excess functional by

$$\Omega_{\rm exc}[\rho]=\Omega_s[\rho]-\Omega_{\rm id}[\rho]\ , \tag{3}$$

$$\Omega_{\rm id}[\rho]=\beta^{-1}\int d^3r\,\rho(\mathbf{r})\{\ln[\lambda^3\rho(\mathbf{r})]-1\}\ , \tag{4}$$

where λ denotes the thermal wavelength and $\beta=1/(k_BT)$. Later we elaborate on $\Omega_{\rm exc}$; for the moment we take this quantity to be given.

Let us consider a planar crystal-vapor interface with perpendicular z direction. We parametrize $\rho=\rho_\Gamma(\mathbf{r})=\rho(\mathbf{r},\Gamma(z))$ by a set $\Gamma(z)=(b_0(z),b_1(z),\ldots)$ of local-order parameters with $b_0(z)$ denoting the local mean density. For instance, $\Gamma(z)$ may be the set of coefficients in a lattice Fourier expansion of $\rho(\mathbf{r})$. The next and crucial premise is that the functions $b_j(z)$ vary smoothly over the domain of short-range order, which is the range of the direct correlation function (DCF)

$$c^{(2)}(\mathbf{r},\mathbf{r}';\Gamma)=-\beta\frac{\delta^2\Omega_{\rm exc}[\rho]}{\delta\rho(\mathbf{r})\delta\rho(\mathbf{r}')}\bigg|_{\rho=\rho_\Gamma}\ . \tag{5}$$

In this case we may perform a gradient expansion[26,33] of $\Omega_s[\rho_\Gamma]$, truncated after terms quadratic in $\dot b_i\equiv db_i/dz$, to arrive at a van der Waals form[30] for the interfacial free energy per unit area,

$$\Sigma=\int_{-\infty}^{+\infty}dz[\tfrac{1}{2}g_{ij}(\Gamma(z))\dot b_i(z)\dot b_j(z)-v(\Gamma(z))] -\tfrac{1}{4}\int_{-\infty}^{+\infty}dz\int_{-\infty}^{+\infty}dz'u(|z-z'|)[b_0(z)-b_0(z')]^2\ , \tag{6}$$

with summation over i and j implied. The matrix g_{ij} is given by

$$g_{ij}(\Gamma)=\frac{k_BT}{2V}\int d^3r\int d^3r'(z-z')^2c^{(2)}(\mathbf{r},\mathbf{r}';\Gamma)\times\frac{\partial\rho(\mathbf{r},\Gamma)}{\partial b_i}\frac{\partial\rho(\mathbf{r}',\Gamma)}{\partial b_j}\ . \tag{7}$$

The term

$$v(\Gamma)=-\Omega(V,T,\mu;[\rho_\Gamma])/V$$

denotes the negative Gibbs functional per unit volume of the bulk system as calculated with spatially *constant* Γ. Finally, $u(z)$ is the tail potential ϕ_l after lateral integration. We note that in the mean-field contribution of the tail potential [second term in Eq. (6)] the global form of the mean density profile $b_0(z)$ enters. The long range of $u(z)$ rules out a gradient expansion in this term.

The variational principle (1) carries over to Σ. The equilibrium density profile is obtained by solving the Euler equations

$$\frac{\delta\Sigma}{\delta\Gamma}=0\ , \tag{8}$$

with the boundary conditions that $\Gamma(z)$ attains the bulk solid or gas value as $z\to\pm\infty$.

Apart from the contribution of the tail potential, the expression (6) for Σ resembles a phenomenological Landau ansatz with a multicomponent order parameter. It should be emphasized, however, that here the coefficient functions are fully specified in terms of practically computable bulk quantities. Qualitative features of surface melting, obtained analytically with a simple model for $v(\Gamma)$ have been described previously.[17,30] Here, we require a more advanced approximation for $\Omega_{\rm exc}(\Gamma)$. A suitable choice is offered by the weighted-density approximation[28,29] (WDA). However, because we need to specify $g_{ij}(\Gamma)$ and $v(\Gamma)$ only for spatially constant[34] order parameters Γ, we gain simplicity in replacing the WDA by its modified version, MWDA, which is likewise based on a spatially constant weighted density.

At this point one may object that the gradient expansion is unnecessary, since the equilibrium form of $\rho_\Gamma(\mathbf{r})$ could be obtained directly from Eq. (1) as soon as we choose a suitable approximation for $\Omega_{\rm exc}$ that supplies coexisting phases. Originally, we indeed followed this seemingly straightforward procedure,[35] using the WDA (Ref. 29) to ensure a realistic DCF for the reference liquid,[36] but the interfacial density profile could not be stabilized. After it was realized[37] that the trouble is due to overlapping hard spheres, we turned to the van der Waals approach where the overlap-problem can be overcome. Moreover, we expect the gradient expansion for $\Gamma(z)$ to be physically justified in the present context, since the crystal-vapor interface near the triple point should display distinct length scales which separate the sharply peaked variation of the local particle density from a comparatively smoother behavior of the order parameters $\Gamma(z)$.

III. APPROXIMATE EXCESS FUNCTIONAL

The MWDA, like the WDA, is based on the premise that a crystal can be viewed as a grossly inhomogeneous liquid with lattice-periodic density $\rho(\mathbf{r})$. In the liquid-based theories of bulk freezing the structure is modeled by a hard-sphere system, which evidently undergoes a liquid-solid transition. The attractive part of ϕ is treated perturbatively.

We follow this practice and replace the potential ϕ_s by a hard core plus a short-range attraction, ϕ_a. To first order in ϕ_a we have

$$\Omega_{\rm exc}[\rho]=\Omega_{\rm HS}[\rho]+\tfrac{1}{2}\int d^3r\int d^3r'\rho(\mathbf{r})\rho(\mathbf{r}')g_{\rm HS}(\mathbf{r},\mathbf{r}',[\rho])\times\phi_a(|\mathbf{r}-\mathbf{r}'|)\ , \tag{9}$$

where $g_{\rm HS}(\mathbf{r},\mathbf{r}',[\rho])$ is the pair-correlation function of the inhomogeneous hard-sphere system. An approximation for $g_{\rm HS}$ in (9) and the choice of the effective hard-sphere diameter d will be specified in Sec. IV. Here we focus attention on $\Omega_{\rm HS}[\rho]$. The input data are the excess free en-

ergy per particle $\psi(\bar{\rho})$ and the DCF, $c_{\rm Hs}(r,\bar{\rho})$, of a uniform hard-sphere liquid with density $\rho(\mathbf{r})\equiv\bar{\rho}$. We employ the Percus-Yevick approximation for *both* quantities in order to ensure consistence with the compressibility sum rule;[31] hence

$$\beta\psi(\bar{\rho})=\tfrac{3}{2}\left[\frac{1}{(1-\eta)^2}-1\right]-\ln(1-\eta)\ , \tag{10}$$

with $\eta=(\pi/6)d^3\bar{\rho}$, and

$$c^{(2)}(r;\bar{\rho})=\begin{cases} a+b\dfrac{r}{d}+a\dfrac{\eta}{2}\left[\dfrac{r}{d}\right]^3, & r\le d \\ 0, & r>d\ , \end{cases}$$
$$a=-\frac{(1+2\eta)^2}{(1-\eta)^4}\ ,\quad b=\frac{6\eta(1+\eta/2)^2}{(1-\eta)^4}\ . \tag{11}$$

The inhomogeneous hard-sphere liquid is now matched to the homogeneous reference system by replacing $\bar{\rho}$ in ψ with a suitably weighted average of the nonuniform density $\rho_\Gamma(\mathbf{r})$. To determine the profiles $\Gamma(z)$, the parameters $b_i\in\Gamma$ should be varied independently within the obvious constraint

$$\int d^3r'\Theta\left[\frac{d}{2}-|\mathbf{r}-\mathbf{r}'|\right]\rho_\Gamma(\mathbf{r}')\le 1\ . \tag{12}$$

A convenient way to incorporate (12) in combination with the Percus-Yevick approximation is offered by the divergence of $\psi(\bar{\rho})$ in the limit $\eta\to 1$, which inhibits configurations violating (12) in the uniform liquid phase. Therefore, we set

$$\psi(\rho)=\hat{\psi}(\rho)+\tilde{\psi}(\rho)\ , \tag{13}$$

$$\tilde{\psi}(\rho)=\begin{cases} 0, & \rho\le\rho_* \\ \psi(\rho)-\Sigma_{\nu=0}^{4}\dfrac{(\rho-\rho^*)^\nu}{\nu!}\dfrac{\partial^\nu\psi}{\partial\rho^\nu}(\rho^*), & \rho_*<\rho<\rho^* \\ \infty, & \rho\ge\rho^*\ , \end{cases} \tag{14}$$

where $\rho^*=6/(\pi d^3)$. We note that $\tilde{\psi}(\rho)$ still diverges as $\rho\to\rho^*$. In (14), ρ_* is an additional parameter that can be chosen conveniently.

The MWDA adapted to the constraint (12) is now introduced by

$$\Omega_{\rm HS}[\rho]=N\hat{\psi}(\hat{\rho})+\int d^3r\,\rho(\mathbf{r})\tilde{\psi}[\bar{\rho}(\mathbf{r})]-\mu N\ , \tag{15}$$

with $N=\int d^3r\,\rho(\mathbf{r})$ and the weighted densities

$$\hat{\rho}=\frac{1}{N}\int d^3r\int d^3r'\rho(\mathbf{r})\rho(\mathbf{r}')\hat{w}(|\mathbf{r}-\mathbf{r}'|;\hat{\rho})\ , \tag{16}$$

$$\bar{\rho}(\mathbf{r})=\rho^*\int d^3r'\Theta\left[\frac{d}{2}-|\mathbf{r}-\mathbf{r}'|\right]\rho(\mathbf{r}')\ . \tag{17}$$

In the spirit of the MWDA, the weight function of $\hat{w}(r,\hat{\rho})$ will be fixed by the condition

$$\left.\frac{\delta^2\Omega_{\rm HS}[\rho]}{\delta\rho(\mathbf{r})\delta\rho(\mathbf{r}')}\right|_{\rho(\mathbf{r})=\bar{\rho}}=-\frac{1}{\beta}c_{\rm HS}(|\mathbf{r}-\mathbf{r}'|,\bar{\rho})\ , \tag{18}$$

together with the normalization

$$\int d^3r\,\hat{w}(|\mathbf{r}-\mathbf{r}'|;\hat{\rho})=1\ . \tag{19}$$

The equations (18) and (19) express the natural requirement that an approximate $\Omega_{\rm HS}[\rho]$ should respect the basic relation (5) in the known case of a homogeneous liquid. When $\bar{\rho}$ approaches ρ^*, then $\Omega_{\rm exc}[\rho]$ increases indefinitely and remains infinite for $\bar{\rho}>\rho^*$. Consequently, configurations violating (12) are suppressed by the cost in free energy. On the other hand, if we set $\rho_*=\rho^*$ and $\tilde{\psi}\equiv 0$, we are back at the original MWDA. Since its weight function does not tend towards a step function when $\hat{\rho}\to\rho^*$, the MWDA fails[38] to account for the constraint (12). In the previous MWDA calculations[31] the problem with (12) is bypassed by the constraint of fixed mean density. In the present case the spatially varying mean density must interpolate between the solid and the vapor phase and thus changes significantly across the interface. Our device to deal with (12) is linked with the Percus-Yevick form of $\psi(\bar{\rho})$ and somewhat ad hoc, but computationally natural and it does not spoil the simplicity of the MWDA. Table I compares results for coexisting densities at the hard-sphere freezing transition, obtained from the unconstrained MWDA and with the above modification for the choice $\rho_*=0.99\rho^*$.

It should be mentioned that the MWDA has a deficiency which also infects its modification proposed here: The DCF of the hard-sphere solid $c(\mathbf{r},\mathbf{r}';[\rho_\Gamma])$ deduced from the approximate $\Omega_{\rm exc}[\rho]$ has oscillatory terms which do not decay as $|\mathbf{r}-\mathbf{r}'|$ increases. However, the amplitudes are inversely proportional to the crystal

TABLE I. Hard-sphere coexisting liquid and solid densities, ρ_{0l},ρ_{0s}, fcc lattice constant a_0, number of particles per unit cell, $2a_0^3\rho_{0s}$, and localization parameter α [see Eq. (25)] for three different versions of MWDA: (1) original version without constraint, (2) original version with constraint $2a_0^3\rho_{0s}=1$, and (3) our adapted version with $\rho_*=0.99\rho^*$. Here we have used the Carnahan-Starling equation of state for the liquid. The data in row 2 differ somewhat from the original work (Ref. 31) since we took more reciprocal lattice shells to evaluate the solid density.

Adapted version	Constraint	$\rho_{0l}d^3$	$\rho_{0s}d^3$	a_0/d	$2a_0^3\rho_{0s}$	αd^2
No	No	0.8292	1.2444	0.8074	1.3100	160.9
No	Yes	0.9119	1.0436	0.7825	1	130.1
Yes	No	0.9208	1.0453	0.7795	0.9902	136.4

volume and the oscillations tend to average out in integrals such as in (7); therefore, we shall ignore these oscillations.

IV. ATTRACTIVE INTERACTION AND PHASE DIAGRAM

The interatomic forces have previously been split into several pieces, which we specify now in more detail. We start with the Lennard-Jones potential

$$\phi_{\mathrm{LJ}}(r)=4\varepsilon\left[\left[\frac{\sigma}{r}\right]^{12}-\left[\frac{\sigma}{r}\right]^{6}\right] . \tag{20}$$

For distances $r<r_0$, with r_0 in the range[30] between 2σ and 3σ, $\phi(r)$ can be approximated by the sum of two Yukawa potentials. This fit[39] is used to represent $\phi_s(r)$. The long-range part $\phi_l(r)$ is then defined by

$$\phi_l(r)=\begin{cases}\phi_{\mathrm{LJ}}(r)-\phi_s(r), & r\geq r_0\\ \phi_{\mathrm{LJ}}(r_0)-\phi_s(r_0), & r<r_0\end{cases} . \tag{21}$$

In the subsequent numerical computation we took $r_0=2.79\sigma$.

With the potential (20), our theory is applicable primarily to rare gases but we also have the option to dismiss Eq. (21) and to consider $\phi_l(r)$ to be an independent microscopic input. In particular, we may set $\phi_l(r)=0$ to examine systems governed by short-range forces only.

As discussed previously, the potential $\phi_s(r)$ will be replaced by a hard-core repulsion and a residual short-range attractive part $\phi_a(r)$. In order to obtain an explicit expression for the contribution of $\phi_a(r)$ in Eq. (9), we adopt approximations introduced by Curtin and Ashcroft,[40] yielding

$$\Omega_{\mathrm{exc}}[\rho]=\Omega_{\mathrm{HS}}[\rho]+\frac{V}{2}\rho_0^2\int d^3r\, g_{\mathrm{HS}}(r;\rho_0)\phi_s(r)$$
$$+\tfrac{1}{2}\int d^3r\int d^3r'[\rho(\mathbf{r})-\rho_0][\rho(\mathbf{r}')-\rho_0]\phi_a(|\mathbf{r}-\mathbf{r}'|)\Theta(|\mathbf{r}-\mathbf{r}'|-r_{nn}/2), \tag{22}$$

with

$$\phi_a(r)=\begin{cases}\phi_s(r), & r\geq 2^{(1/6)}\sigma\\ -\varepsilon, & r<2^{(1/6)}\sigma\end{cases} . \tag{23}$$

In Eq. (22), the pair-correlation function $g_{\mathrm{HS}}(r;\rho_0)$ of a homogeneous hard-sphere fluid with mean density ρ_0 enters, for which we use the Verlet-Weis expression[41] with an effective hard-sphere diameter,[42]

$$d(T)=\int_0^\infty dr(1-e^{-\beta\phi_s(r)}) . \tag{24}$$

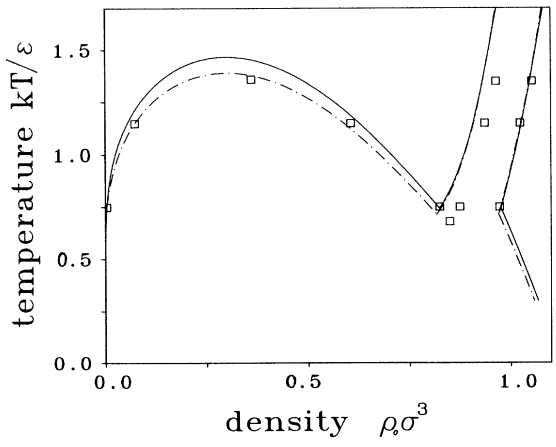

FIG. 1. Bulk phase diagram for a Lennard-Jones system without (dash-dotted line) and with (solid line) long-range potential tail. Squares denote simulation data (Ref. 43) for a truncated Lennard-Jones potential.

The step function in (22), with $r_{nn}\equiv\sqrt{2}a_0$ denoting the interparticle spacing in the solid, avoids self-interaction effects.[40]

In employing the approximation (22) for $\Omega_{\mathrm{exc}}[\rho]$ the main difference with Ref. [40] is in $\Omega_{\mathrm{HS}}[\rho]$; here we take the MWDA for $\Omega_{\mathrm{HS}}[\rho]$ instead of the WDA, for reasons mentioned in Sec. III.

To determine the bulk phase diagram we parametrize the local density as

$$\rho(\mathbf{r})=2a_0^3\rho_0\left[\frac{\alpha}{\pi}\right]^{3/2}\sum_{\mathbf{R}}\exp[-\alpha(\mathbf{r}-\mathbf{R})^2] , \tag{25}$$

where $\{\mathbf{R}\}$ label the sites of an fcc lattice; the volume of the elementary cell is $2a_0^3$.

With the input data provided by MWDA, we minimized the grand canonical free energy with respect to the three parameters a_0, ρ_0, and α. The result is shown in Fig. 1, which also displays the dependence of the phase diagram on the long-range tail of the Lennard-Jones potential, $\phi_l^{\mathrm{LJ}}(r)$. The values of the critical and triple-point temperature turn out to be $k_BT_c=1.47\varepsilon$ (1.39ε) and $k_BT_t=0.74\varepsilon$ (0.71ε), with the values in brackets holding for $\phi_l=0$.

Compared to simulation results[43] ($k_BT_c=1.36\varepsilon$, $k_BT_t=0.68\varepsilon$) for Lennard-Jones potential truncated at $r=2.5\sigma$, and experimental data for Argon[44] ($k_BT_c=1.26\varepsilon$, $k_BT_t=0.7\varepsilon$), both the critical temperatures and the triple-point temperatures are reproduced satisfactorily.

V. INTERFACIAL PROFILES: SURFACE MELTING

We examine now the solid-vapor interface when the temperature is raised along the sublimation line towards

the triple point. The occurrence of surface melting will be inferred from the interfacial profiles of local mean density and crystalline order.

These profiles are obtained by solving the Euler equations (8), which read explicitly,

$$g_{ij}\ddot{b}_j+\Gamma_{ijk}\dot{b}_j\dot{b}_k=-\frac{\partial v}{\partial b_i}+K\delta_{i0}\ , \tag{26}$$

where $\dot{b}_i=db_i/dz$ and

$$2\Gamma_{ijk}=\frac{\partial g_{ij}}{\partial b_k}+\frac{\partial g_{ki}}{\partial b_j}-\frac{\partial g_{jk}}{\partial b_i}\ , \tag{27}$$

$$K(z)=\int_{-\infty}^{+\infty}dz'u(|z-z'|)[b_0(z')-b_0(z)]\ . \tag{28}$$

We also note that

$$v(\Gamma)=v_s(\Gamma)-\tfrac{1}{2}b_0^2\int d^3r\,\phi_l(r)\ , \tag{29}$$

with $v_s(\Gamma)$ deriving from $\phi_s(r)$.

It is seen from the expansion (6) and the Euler equations that $\Sigma(\Gamma)$ may be interpreted as the dynamical action of a fictitious particle moving in Γ space with mass tensor $g_{ij}(\Gamma)$ and potential energy $v(\Gamma)$. The coordinate z plays the role of a time variable. This analogy[30] is particularly intuitive and useful in the case $\phi_l=0$, where the "memory" term K vanishes and "energy conservation" yields immediately a first integral of motion.

To solve Eq. (26) we take over Eq. (25) with the parameters now depending on z,

$$\rho(\mathbf{r},\Gamma(z))=2a_0^3\rho_0(z)\left[\frac{\alpha(z)}{\pi}\right]^{3/2}\times\sum_{\mathbf{R}}\exp[-\alpha(z)(\mathbf{r}-\mathbf{R})^2]\ , \tag{30}$$

where a_0 is the temperature-dependent but z-independent lattice constant of the fcc crystal. The parametrization comprises lattice Fourier coefficients of arbitrary order. It will be convenient to replace the variable $\alpha(z)$ by the Fourier coefficient

$$\chi(z)=\rho_0(z)\exp\left[-\frac{G_1^2}{4\alpha(z)}\right]\ , \tag{31}$$

with $\mathbf{G}_1$ a basis vector of the reciprocal lattice $G_1^2=3\pi^2/a_0^2$. With the ansatz (30) we truncate Γ to a two-dimensional space, so that $\Gamma(z)=(b_0(z)=\rho_0(z), b_1(z)=\chi(z))$ involves the local mean density $\rho_0(z)$ and the crystallinity $\chi(z)$. We note that the Γ space is restricted by the inequality $\chi(z)\le\rho_0(z)$. The graphs of $v_s(\Gamma)$ and $g_{ij}(\Gamma)$ are displayed in Figs. 2 and 3 for solid-vapor coexistence at the reduced temperature $t=(T_t-T)/T_t=0.015$. The potential $v_s(\Gamma)$ exhibits two peaks of equal height corresponding to bulk solid and gas, and a lower peak for the incipient liquid. The mass tensor $g_{ij}(\Gamma)=g_{ji}(\Gamma)$ is seen to vary significantly with the order parameters. This finding casts doubts on the quantitative features of models[17,18,30] with constant g_{ij}. We solved Eqs. (26) numerically with a shooting method, starting at the gas peak and selecting those trajectories which reach the solid peak.

Let us first consider short-range forces. For this case and for two order parameters it has been proven[30] that the number of solutions is odd. The physically realized trajectory (i.e., profile) is that one with minimal action (i.e., surface tension). Here, we find that there is only one trajectory connecting the gas peak with the solid peak, and it approaches the liquid peak as $t\to0$. Therefore, this solution describes complete surface melting.

In Figs. 4(a)–4(c) the local mean density $\rho_0(z)$ and the crystallinity $\chi(z)$ are shown for the reduced temperatures $t_a=0.3433$, $t_b=0.0149$, and $t_c=1.2\times10^{-4}$. The profiles are independent of the interface orientation. In order to detect a possible orientational dependence of surface melting, one has to include additional crystal order parameters allowing, for example, the width of the density peaks in Eq. (30) to become anisotropic.

In Figs. 5(a)–5(c) we plotted profiles of the laterally integrated density

$$\bar{\rho}(z)=\frac{1}{A}\int\int_A dx\,dy\,\rho(x,y,z) \tag{32}$$

for the (110) interface (area A). $\bar{\rho}(z)$ varies with the orientation of the interface for purely geometrical reasons. The onset of crystalline order separates from the rise of local mean density on the vapor side and a quasi-liquid layer grows progressively as $t\to0$. The incipient liquid-solid interface moves to the right without discernible change in its shape.

At the triple point $k_BT_t=0.71\varepsilon$ ($\phi_l=0$) the (10-90) width in the gas-liquid interface is 2.1 σ. Its surface tension is found to be $1.04\varepsilon/\sigma^2$. By extrapolation of simulation data[45] to the above value of T_t, we find $1.5\pm0.3\sigma$ and $0.9\pm0.25\varepsilon/\sigma^2$, respectively. For the width of the liquid-solid interface at $T_t(\phi_l=0)$ we obtain the value 2.0 σ and a surface tension of 0.57 ε/σ^2, whereas computer

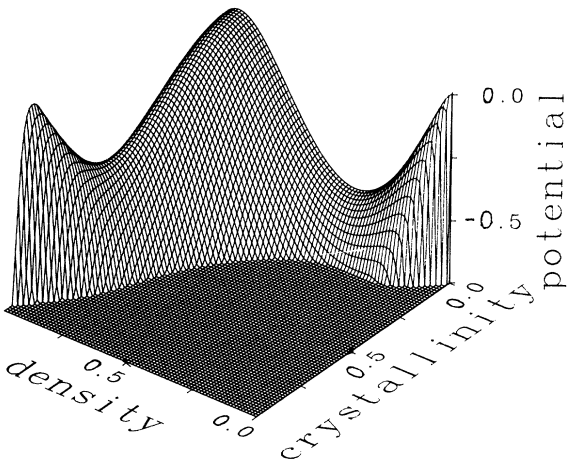

FIG. 2. Potential $v_s(\Gamma)\sigma^3/\beta$ vs order parameters $\rho_0\sigma^3$ and $\chi\sigma^3$.

simulations[20] yield the surface tension to be $0.35\pm0.03\varepsilon/\sigma^2$, very slightly depending on orientation. This discrepancy may be due in part to the gradient expansion for $\Sigma(\Gamma)$, which is known[46] to overestimate, as a rule, the liquid-solid surface tension.

Finally, we turn to the effect of long-range forces with potential ϕ_l^{LJ}. We find that the interfacial widths and the surface tensions are not altered significantly but the increase in thickness of the quasiliquid layer is substantial, as can be seen in Fig. 6. For example, at $t_0=2.5\times10^{-3}$ we obtain a thickness $L_0=3.0\sigma$ for $\phi_l=0$, while $L_0=4.6\sigma$ in the case of long-range forces. The latter value of L_0 corresponds to about eight molten (110) layers and agrees satisfactorily with the experimental results from argon films.[3] The effect of ϕ_l on the thickness $L(t)$ of the wetting layer illustrates the general result[13,16,17,30] that long-range forces induce a change from a logarithmic to an algebraic growth law for the asymptotic behavior of $L(t\rightarrow0)$.

A glance at Figs. 4 and 5 might provoke the impression that the incipient liquid grows exclusively at the expenses of the crystalline order, implying that no solid phase is left at the triple point. This conclusion would be unwarranted, however. The point is that the Euler equations are translation-invariant. Hence, if $\Gamma(z)$ solves Eq. (8), then $\Gamma_a(z)\equiv\Gamma(z+a)$ is also a solution. In other words,

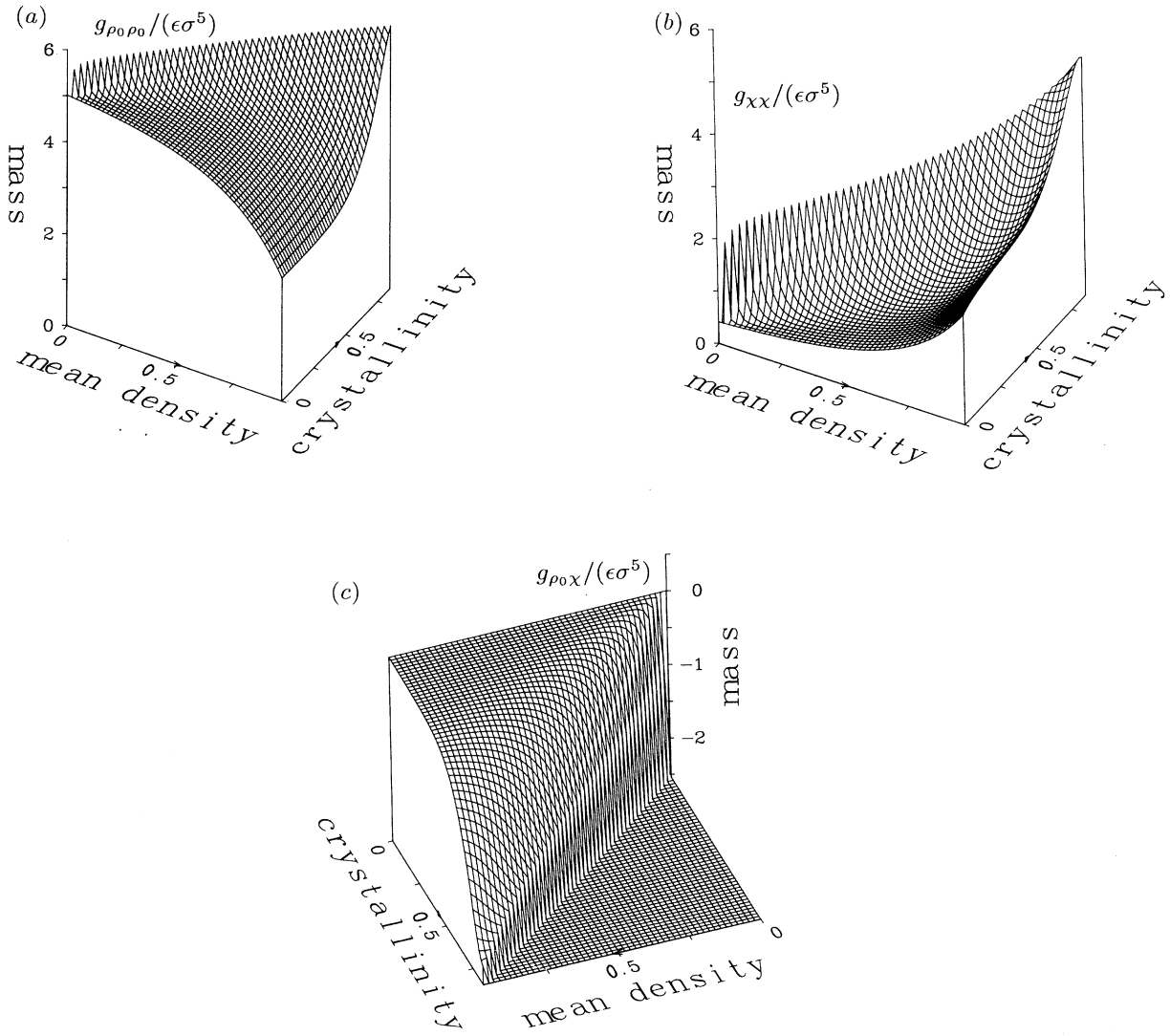

FIG. 3. Mass tensor $g_{ij}(\Gamma)/(\varepsilon\sigma^5)$ vs order parameters $\rho_0\sigma^3$ and $\chi\sigma^3$. (a) $g_{\rho_0\rho_0}/(\varepsilon\sigma^5)$, (b) $g_{\chi\chi}/(\varepsilon\sigma^5)$, (c) $g_{\rho_0\chi}/(\varepsilon\sigma^5)$.

the shift in the position of the entire interface corresponds to a zero mode without costs in free energy. We have tacitly and arbitrarily fixed the origin of the z axis at the vapor side of the interfacial layer. We could do otherwise and put, for instance, the origin on the solid side, so that surface melting of the crystal would turn into surface condensation of the vapor.

In practice, the ultimate positions of the vapor-liquid and liquid-solid interfaces at the triple point are governed by symmetry-breaking constraints (leading to finite-size

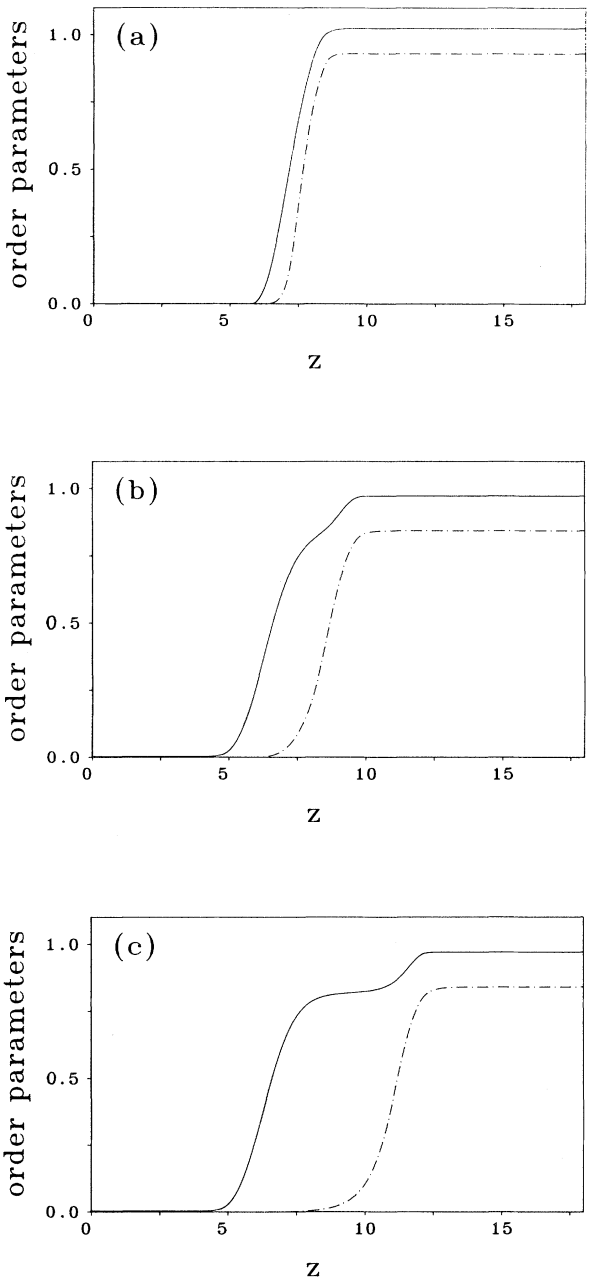

FIG. 4. Order-parameter profiles $\rho_0(z)\sigma^3$ (solid line), $\chi(z)\sigma^3$ (dash-dotted line) for solid-vapor coexistence situations near the triple point of a Lennard-Jones system without long-range tail. We choose three different reduced temperatures (a) $t=0.3433$, (b) $t=0.0149$, (c) $t=1.2\times10^{-4}$.

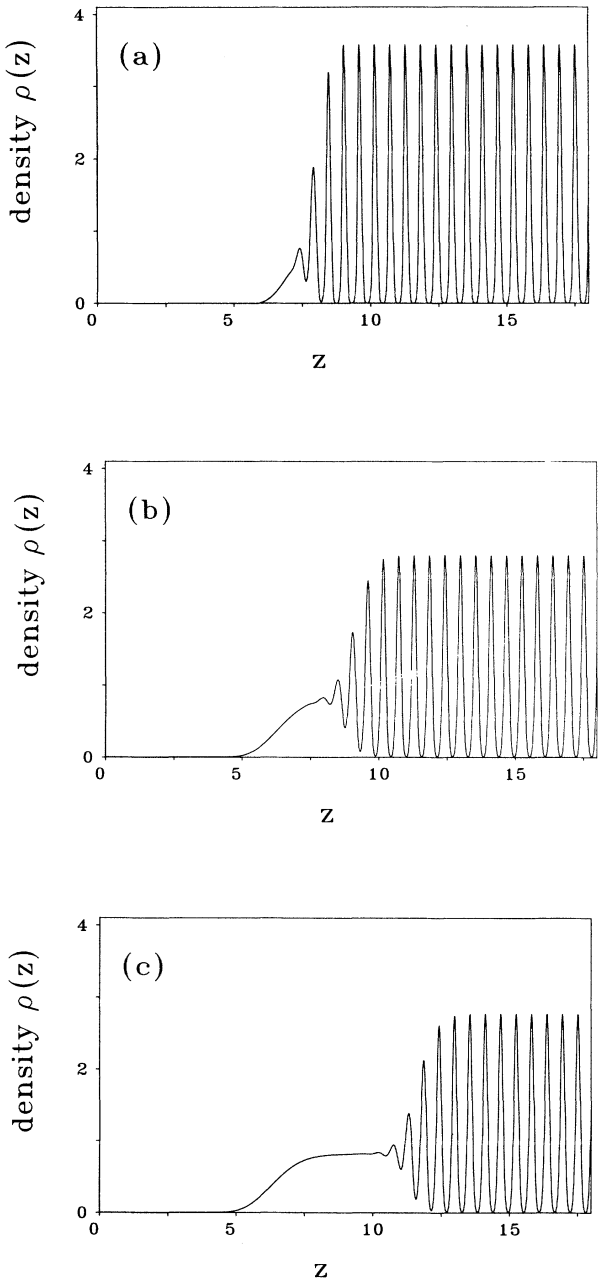

FIG. 5. The laterally integrated density $\bar{\rho}(z)\sigma^3$ in (110) orientation at the same temperatures as in Fig. 4.

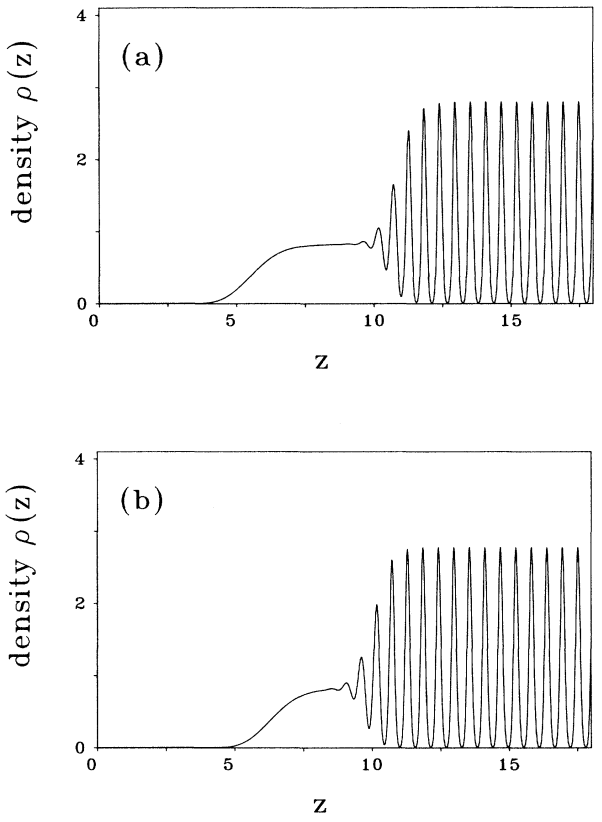

FIG. 6. Same as Fig. 5 at the reduced temperature $t=2.5\times10^{-3}$, but now (a) with long-range tail compared to a profile (b) without long-range tail at same t.

effects[47,48]) or by external fields[49] (e.g., wall potentials) which couple to the zero mode. These interactions are crucial in controlling the latent heat, i.e., the relative amount of coexisting phases at the triple point.

VI. CONCLUSIONS AND OUTLOOK

We made an attempt to link up surface melting with the current theory of bulk freezing in simple fluids. Using density-functional techniques combined with a gradient expansion, we arrive at a van der Waals form for the free energy of a planar interface, which requires the pairwise atomic potential and the lattice structure as the sole essential input data for computing interfacial profiles. The results for a Lennard-Jones potential, in particular, display a steadily growing molten layer near the triple point. Long-range forces increase the layer thickness significantly up to a value that is in good agreement with measurements on argon.

The microscopic theory presented here captures features of surface melting and makes contact with previous phenomenological approaches. But, of course, there is room for future improvements. Some of these are presumably straightforward although they will afford more extensive computer work than was necessary here. To explore the anisotropy of surface melting and to allow for near-surface relaxation of the crystal lattice, additional crystal order parameters must be included.

Attempts to go beyond the gradient expansion while keeping the link between the short-range order in the liquid with that in the solid raise tougher questions. On the other hand, our results are not inconsistent with the smoothness assumption underlying the gradient expansion. Moreover, the latter gives an intuitive picture for surface melting on the basis of realistic bulk phases and provides a starting point to explore the effects of capillary fluctuations and local lattice defects upon the formation of the quasiliquid layer.

ACKNOWLEDGMENTS

We thank T. Beier for many discussions and for supplying us with several computer programs. This work was supported by the Bundesministerium für Forschung und Technologie (BMFT) under Contract No. 03WA2LMU.

[1]A review is J. G. Dash, Comtemp. Phys. **30**, 89 (1989).
[2]G. Tammann, Z. Phys. Chem. **68**, 205 (1910); I. N. Stranski, Naturwissenschaften **28**, 30 (1942).
[3]D. M. Zhu and J. G. Dash, Phys. Rev. Lett. **57**, 2959 (1986); **60**, 432 (1988).
[4]K. D. Stock, Surf. Sci. **91**, 665 (1980).
[5]J. W. M. Frenken and J. F. van der Veen, Phys. Rev. Lett. **54**, 134 (1985).
[6]J. W. M. Frenken, P. M. J. Maree, and J. F. van der Veen, Phys. Rev. B **34**, 7506 (1986).
[7]B. Pluis, A. W. Denier van der Gon, J. W. M. Frenken, and J. F. van der Veen, Phys. Rev. Lett. **59**, 2678 (1987).
[8]B. Pluis, T. N. Taylor, D. Frenkel, and J. F. van der Veen, Phys. Rev. B **40**, 1353 (1989).
[9]K. C. Prince, U. Breuer, and H. P. Bonzel, Phys. Rev. Lett. **60**, 1146 (1988).
[10]B. Pluis, J. M. Gay, J. W. M. Frenken, S. Gierlotka, J. F. van der Veen, J. E. MacDonalds, A. A. Williams, N. Piggins, and J. Als-Nielsen, Surf. Sci. **222**, L845 (1989).
[11]J. Daeges, H. Gleiter, and J. H. Perpezko. Phys. Lett. **119A**, 79 (1986).
[12]L. Pietronero and E. Tosatti, Solid State Commun. **32**, 255 (1979).
[13]A. Trayanov and E. Tosatti, Phys. Rev. Lett. **59**, 2207 (1987); Phys. Rev. B **38**, 6961 (1988).
[14]Guozhong An and M. Schick, Phys. Rev. B **39**, 9722 (1989).
[15]R. T. Lyzhva, A. Y. Mitus, and A. Z. Patashinskii, Zh. Eksp. Teor. Fiz. **81**, 2198 (1981) [Sov. Phys.—JETP **54**, 1168 (1981)].
[16]R. Lipowsky and W. Speth, Phys. Rev. B **28**, 3983 (1983).
[17]A. C. Levi and E. Tosatti, Surf. Sci. **189/190**, 641 (1987).
[18]R. Lipowsky, U. Breuer, K. C. Prince, and H. P. Bonzel, Phys. Rev. Lett. **62**, 913 (1989).
[19]T. Yamamoto and T. Izuyama, J. Phys. Soc. Jpn. **57**, 3742 (1988).
[20]J. Q. Broughton and L. V. Woodcock, J. Phys. C **11**, 2743

(1986); J. Q. Broughton and G. H. Gilmer, J. Chem. Phys. **79**, 5095 (1983); **79**, 5105 (1983); **79**, 5119 (1983).
[21]W. Schommers, Phys. Rev. B **32**, 6845 (1985).
[22]V. Rosato, G. Ciccotti, and V. Pontikis, Phys. Rev. B **33**, 1860 (1986).
[23]S. Valkealahti and R. Nieminen, Phys. Scr. **36**, 646 (1987).
[24]P. Stoltze, J. K. Nørskov, and U. Landman, Phys. Rev. Lett. **61**, 440 (1988).
[25]E. T. Chen, R. N. Barnett, and U. Landman, Phys. Rev. B **40**, 924 (1989).
[26]See, e.g., R. Evans, Adv. Phys. **28**, 143 (1979).
[27]See, e.g., A. D. J. Haymet, Prog. Solid State Chem. **17**, 1 (1986); M. Baus, J. Stat. Phys. **48**, 1129 (1987).
[28]P. Tarazona, Phys. Rev. A **31**, 2672 (1985).
[29]W. A. Curtin and N. W. Ashcroft, Phys. Rev. A **32**, 2909 (1985).
[30]H. Löwen, T. Beier, and H. Wagner, Europhys. Lett. **9**, 791 (1989); Z. Phys. B **79**, 109 (1990).
[31]A. R. Denton and N. W. Ashcroft, Phys. Rev. A **39**, 4701 (1989).
[32]This problem has already been mentioned by W. A. Curtin and K. Runge, Phys. Rev. A **35**, 4755 (1987); see also J. Percus, J. Stat. Phys. **52**, 1157 (1988).
[33]A. D. J. Haymet and D. W. Oxtoby, J. Chem. Phys. **74**, 2559 (1989); D. W. Oxtoby and A. D. J. Haymet, *ibid.* **76**, 6262 (1982).
[34]The dependence of Γ on the variable Z, i.e., the order-parameter profile, arises from solving the Euler equations (8).
[35]W. A. Curtin, Phys. Rev. Lett. **59**, 1228 (1987); Phys. Rev. B **39**, 6775 (1989).
[36]After this work was completed we became aware of the paper by T. A. Cherepanova and A. V. Stekolnikov, J. Cryst. Growth **99**, 88 (1990), dealing with surface melting within a primitive version of the WDA. The authors avoid the gradient expansion but they use a simple step function for the weighted density which is known[28] to be a quantitatively poor description of the liquid strucuture.
[37]T. Beier (private communication); see also T. Beier, H. Löwen, and H. Wagner (unpublished).
[38]The procedure employed here is inapplicable to inhibit hard-core overlap in the WDA. The nonlinear differential equation for the WDA weight function resulting from Eq. (13) for $\psi(\rho)$ does not yield a stable solution. In the work of Ref. 35, the problem of overlapping hard spheres is bypassed by a constrained density parametrization.
[39]S. M. Foiles and N. W. Ashcroft, J. Chem. Phys. **75**, 3594 (1981).
[40]W. A. Curtin and N. W. Ashcroft, Phys. Rev. Lett. **56**, 2776 (1986).
[41]L. Verlet and J. J. Weis, Phys. Rev. A **5**, 939 (1972).
[42]J. A. Barker and D. Henderson, J. Chem. Phys. **47**, 4714 (1967).
[43]L. Verlet and D. Levesque, Physica **36**, 245 (1967); J. P. Hansen and L. Verlet, Phys. Rev. **184**, 151 (1969).
[44]A. M. Clark, F. Din, J. Roob, A. Michels, A. Wasendar and T. N. Zwietering, Physica **17**, 876 (1951).
[45]For a compilation of references, see, e.g., B. Q. Lu, R. Evans, and M. M. Telo da Gama, Mol. Phys. **55**, 1319 (1985).
[46]W. McMullen and D. W. Oxtoby, J. Chem. Phys. **88**, 1967 (1988).
[47]R. Lipowsky and G. Gompper, Phys. Rev. B **29**, 5213 (1984).
[48]G. Gompper and D. M. Kroll, Phys. Rev. B **40**, 7221 (1989); see also H. Löwen, Surf. Sci. **234**, 315 (1990).
[49]H. Löwen and T. Beier, Z. Phys. B **79**, 441 (1990).